An Instantaneous Active and Reactive Current Component Method for Active Filters

Vasco Soares, Pedro Verdelho, *Member, IEEE*, and Gil D. Marques, *Member, IEEE*

***Abstract*—A shunt active filter based on the instantaneous active and reactive current component i_d-i_q method is proposed. This new control method aims to compensate harmonics and first harmonic unbalance. To evaluate its relative performance it is compared with the instantaneous active and reactive power p-q method under various mains voltage conditions and for different harmonic injection high-pass filters. Both methods are completely frequency-independent, however under distorted mains voltages the proposed method presents a better harmonic compensation performance. The system synthesis and implementation are performed. Simulation and experimental results are presented.**

***Index Terms*—Active Filters, id-iq method, p-q method.**

I. Introduction

STATIC power converters such as single-phase and three-phase rectifiers, thyristor converters and a large number of low-power electronic-based appliances, are nonlinear loads that generate considerable disturbance in the ac mains. Current harmonics, which may also be asymmetric, cause voltage drops across the supply network impedance as well as other undesirable phenomena (e.g. shunt and series resonance, flicker) resulting in distorted supply voltages, and hence a reduction in the supply voltage quality. These problems can be ever worse in small power networks where impedance may be significant resulting in increasing voltage distortion at the point of common coupling (PCC). In general, the supply harmonic current content is constantly changing due to load current needs and the random nature of network topology. Many kinds of nonlinear loads such as welding equipment, arc furnaces and motor drives with fast dynamics generate a random harmonic current content. As a result, conventional solutions that rely on passive filters to perform a harmonic reduction are ineffective. Under these conditions it has been proved that the most effective solutions are active filters (AF's) which are able to compensate not only harmonics but also asymmetric currents caused by nonlinear and unbalanced loads. Due to the remarkable progress in the last two decades in the field of power electronics devices with forced commutation, AF's have been extensively studied and a large number of works have been published [1]–[9]. One type of AF widely used is the shunt type AF that relies on a three-leg voltage source converter (VSC) (Fig. 1).

AF behavior under sinusoidal and balanced conditions has already been analyzed. However the mains voltages at the PCC may be unbalanced and even nonsinusoidal. It is therefore very important to study the behavior of AF's under such voltage conditions, and ascertain the most advisable control strategy to achieve the current compensation. This can be realized by simulation of the AF with different control strategies and considering different voltage conditions in order to study their influence.

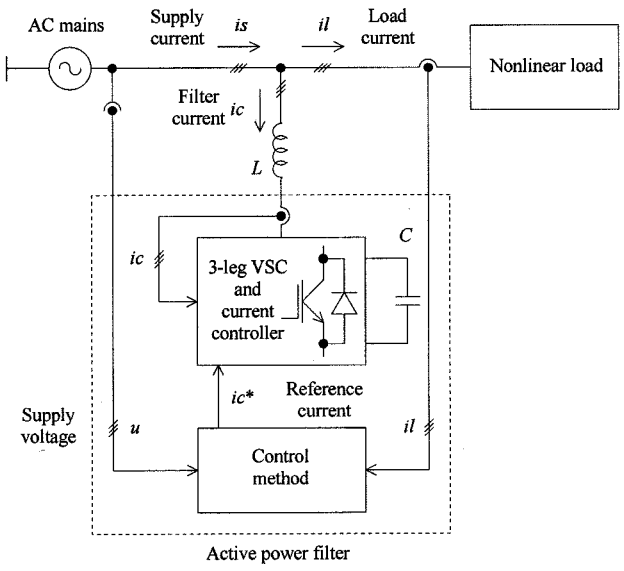

Fig. 1. Basic structure of a shunt AF with a three-leg VSC.

In this paper an AF control method is presented. This control method has been named the "Instantaneous active and reactive current component i_d-i_q method" [6]. The AF performance for the well-known instantaneous active and reactive power p-q method [1] and the proposed i_d-i_q control method is evaluated with respect to the mains harmonic current content, and high-pass filter effectiveness under various mains voltage conditions. Both methods are compared under distorted mains voltage conditions and it is shown that the i_d-i_q control method achieves a superior harmonic compensation performance. The i_d-i_q control method is based on a synchronous rotating frame derived from the mains voltages without the use of a phase-locked loop (PLL). A large number of AF's are implemented with a PLL [5], [9], so using the i_d-i_q control method many synchronization problems are avoided and a truly frequency-independent filter is achieved.

II. Control Methods and Ideal Steady State Analysis

In this section two control methods are described as well as their ideal analysis in steady state conditions. In this analysis it

Manuscript received December 11, 1998; revised December 20, 1999. Recommended by Associate Editor, P. K. Jain.

The authors are with the Department of Electrical and Computer Engineering, Instituto Superior Tecnico, Lisboa 1049-001, Portugal (e-mail: vesoares@iscl.ipl.pt; pcverdelho@alfa.ist.utl.pt; gmarques@alfa.ist.utl.pt).

Publisher Item Identifier S 0885-8993(00)05571-X.

is assumed that the VSC is a zero-order system with a unitary transfer function, so the converter currents ic_i, where i stands for the phase number, instantaneously follow the reference currents ic_i^*. In Section II-A, the well-known instantaneous active and reactive power p-q method is briefly explained. In Section II-B the proposed instantaneous active and reactive current component i_d-i_q method is presented. A comparison between the two control methods is given in Section II-C. Finally, a steady state analysis using fast Fourier transform (FFT) which allows the performance of these control methods to be evaluated under different voltage conditions is presented in Section II-D.

A. Instantaneous Active and Reactive Power p-q Method

The active filter currents ic_i are obtained from the instantaneous active and reactive powers pl and ql of the nonlinear load. This is achieved by previous calculation of the mains voltages u_i and the nonlinear load currents il_i in a stationary reference frame, i.e., in $\alpha\beta$ components by (1) and (2). A null value for the zero voltage component is assumed. The zero current component is also null since the absence of neutral wire is considered

$$\begin{bmatrix} u_\alpha \\ u_\beta \end{bmatrix} = \sqrt{\frac{2}{3}} \cdot \begin{bmatrix} 1 & -1/2 & -1/2 \\ 0 & \sqrt{3}/2 & -\sqrt{3}/2 \end{bmatrix} \cdot \begin{bmatrix} u_1 \\ u_2 \\ u_3 \end{bmatrix} \quad (1)$$

$$\begin{bmatrix} il_\alpha \\ il_\beta \end{bmatrix} = \sqrt{\frac{2}{3}} \cdot \begin{bmatrix} 1 & -1/2 & -1/2 \\ 0 & \sqrt{3}/2 & -\sqrt{3}/2 \end{bmatrix} \cdot \begin{bmatrix} il_1 \\ il_2 \\ il_3 \end{bmatrix}. \quad (2)$$

The instantaneous active and reactive load powers pl and ql are defined by [1] as

$$\begin{bmatrix} pl \\ ql \end{bmatrix} = \begin{bmatrix} u_\alpha & u_\beta \\ u_\beta & -u_\alpha \end{bmatrix} \cdot \begin{bmatrix} il_\alpha \\ il_\beta \end{bmatrix} \quad (3)$$

which can be decomposed into oscillatory and average terms $pl = \tilde{pl} + Pl$, and $ql = \tilde{ql} + Ql$. Under balanced and sinusoidal mains voltage conditions the average power components are related to the first harmonic current of positive sequence, il_{1h}^+, and the oscillatory components represent all higher order current harmonics including the first harmonic current of negative sequence, $il_{nh}^{\pm} + il_{1h}^-$. Thus, the AF should compensate the oscillatory power components so that the average power components remain in the mains. In this way the power rating of the AF is minimum. After eliminating the average power components by high-pass filters (HPF) the powers to be compensated are $pc = -\tilde{pl}$ and $qc = -\tilde{ql}$. The compensation currents are obtained by inverting the matrix in (3). These currents may be calculated by (4) and (5)

$$\begin{bmatrix} ic_\alpha \\ ic_\beta \end{bmatrix} = \frac{1}{u_\alpha^2 + u_\beta^2} \begin{bmatrix} u_\alpha & u_\beta \\ u_\beta & -u_\alpha \end{bmatrix} \cdot \begin{bmatrix} pc \\ qc \end{bmatrix} \quad (4)$$

$$\begin{bmatrix} ic_1 \\ ic_2 \\ ic_3 \end{bmatrix} = \sqrt{\frac{2}{3}} \cdot \begin{bmatrix} 1 & -1/2 & -1/2 \\ 0 & \sqrt{3}/2 & -\sqrt{3}/2 \end{bmatrix}^T \cdot \begin{bmatrix} ic_\alpha \\ ic_\beta \end{bmatrix}. \quad (5)$$

B. Instantaneous Active and Reactive Current Component i_d-i_q Method

In this method the currents ic_i are obtained from the instantaneous active and reactive current components il_d and il_q of the nonlinear load. In the same way, the mains voltages u_i and the polluted currents il_i in $\alpha\beta$ components must be calculated as in the previous method by (1) and (2). However, the dq load current components are derived from a synchronous reference frame based on the Park transformation, where θ represents the instantaneous voltage vector angle (6)

$$\begin{bmatrix} il_d \\ il_q \end{bmatrix} = \begin{bmatrix} \cos\theta & \sin\theta \\ -\sin\theta & \cos\theta \end{bmatrix} \cdot \begin{bmatrix} il_\alpha \\ il_\beta \end{bmatrix}, \quad \theta = \tan^{-1}\frac{u_\beta}{u_\alpha}. \quad (6)$$

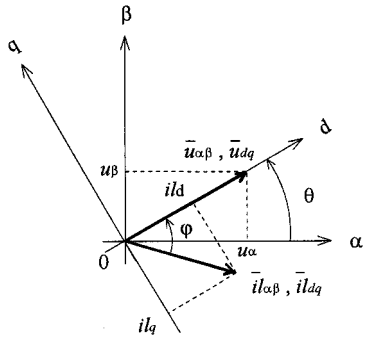

Fig. 2. Voltage and current space vectors in the stationary and synchronous reference frames.

Fig. 2 depicts the voltage and current space vectors in the stationary $(\alpha\beta)$ and rotating frames (dq). Under balanced and sinusoidal mains voltage conditions angle θ is a uniformly increasing function of time. This transformation angle is sensitive to voltage harmonics and unbalance, therefore $d\theta/dt$ may not be constant over a mains period.

With transformation (6) the direct voltage component is $u_d = |\bar{u}_{dq}| = |\bar{u}_{\alpha\beta}| = \sqrt{u_\alpha^2 + u_\beta^2}$ and the quadrature voltage component is always null, $u_q = 0$, so due to geometric relations (6) becomes

$$\begin{bmatrix} il_d \\ il_q \end{bmatrix} = \frac{1}{\sqrt{u_\alpha^2 + u_\beta^2}} \cdot \begin{bmatrix} u_\alpha & u_\beta \\ -u_\beta & u_\alpha \end{bmatrix} \cdot \begin{bmatrix} il_\alpha \\ il_\beta \end{bmatrix}. \quad (7)$$

Instantaneous active and reactive load currents il_d and il_q can also be decomposed into oscillatory and average terms $il_d = \tilde{il}_d + Il_d$, and $il_q = \tilde{il}_q + Il_q$. The first harmonic current of positive sequence is transformed to dc quantities, il_{dq1h}^+, i.e., this constitutes the average current components. All higher order current harmonics including the first harmonic current of negative sequence, $il_{dqnh}^{\pm} + il_{dq1h}^-$, are transformed to non-dc quantities and undergo a frequency shift in the spectra, and so, constitute the oscillatory current components. These assumptions are valid under balanced and sinusoidal mains voltage conditions. Eliminating the average current components by HPF's the currents that should be compensated are obtained, $ic_d = -\tilde{il}_d$ and $ic_q = -\tilde{il}_q$. Finally, (8) and (5) calculate the converter currents in the system coordinates

$$\begin{bmatrix} ic_\alpha \\ ic_\beta \end{bmatrix} = \frac{1}{\sqrt{u_\alpha^2 + u_\beta^2}} \cdot \begin{bmatrix} u_\alpha & -u_\beta \\ u_\beta & u_\alpha \end{bmatrix} \cdot \begin{bmatrix} ic_d \\ ic_q \end{bmatrix}. \quad (8)$$

One of the characteristics of both methods is that the compensating currents are calculated directly from the mains voltages, enabling the methods to be frequency-independent. Avoiding the use of a PLL a large frequency operating range can be achieved limited chiefly by the cutoff frequency of

the current control system (VSC and current controller). Furthermore, under unbalanced and nonsinusoidal mains voltage conditions, a large number of synchronization problems are avoided especially if a PLL is synthesized with a fast dynamic response.

C. Comparison Between the Control Methods

The active and reactive powers defined in (3) can be given by the inner and external product of the voltage and current space vectors. Because Park's transformation (6) is a simple rotation of angle θ, and is applied to both voltage and current space vectors, the powers pl and ql are invariant under this transformation. This result is not valid for all definitions of reactive power but it is valid for the definition adopted in this paper. As the Park transformation guarantees power invariance a comparison between the two control methods can be performed. This is realized by means of the active and reactive load powers. Therefore, as the reference frame is chosen in such a way that $u_q = 0$, the load powers can be established as

$$\begin{bmatrix} pl \\ ql \end{bmatrix} = u_d \cdot \begin{bmatrix} il_d \\ -il_q \end{bmatrix} \tag{9}$$

which can be decomposed in (10), where U_d and $\tilde{u}_d$ are the average and oscillatory terms of the mains voltages, respectively. The average voltage component is representative of the first harmonic voltage of positive sequence, u_{1h}^{+}. All higher order harmonic voltages as well as unbalance, $u_{nh}^{\pm}+u_{1h}^{-}$, are represented by the oscillatory components

$$\begin{bmatrix} Pl \\ Ql \end{bmatrix} + \begin{bmatrix} \tilde{p}l \\ \tilde{q}l \end{bmatrix} = (U_d + \tilde{u}_d) \cdot \left(\begin{bmatrix} Il_d \\ -Il_q \end{bmatrix} + \begin{bmatrix} \tilde{i}l_d \\ -\tilde{i}l_q \end{bmatrix} \right). \tag{10}$$

In the p-q control method the product of the average values in voltage and currents shown in (10) results in average power components that are eliminated by the HPF's. For the i_d-i_q control method the filtering action is performed over the load current components.

Under balanced and sinusoidal mains voltage conditions the oscillatory voltage component $\tilde{u}_d$ is null, so through relation (10), the equivalent compensation powers for the p-q control method, pc_1 and qc_1, are equal to the equivalent compensation powers derived from the i_d-i_q control method, pc_2 and qc_2 (11)

$$\begin{bmatrix} pc_1 \\ qc_1 \end{bmatrix} = \begin{bmatrix} pc_2 \\ qc_2 \end{bmatrix} = -U_d \cdot \begin{bmatrix} \tilde{i}l_d \\ -\tilde{i}l_q \end{bmatrix}. \tag{11}$$

For unbalanced and nonsinusoidal mains voltage conditions, where $\tilde{u}_d$ should be considered, the equivalent compensation powers are now defined by (12) and (13)

$$\begin{bmatrix} pc_1 \\ qc_1 \end{bmatrix} = -U_d \cdot \begin{bmatrix} \tilde{i}l_d \\ -\tilde{i}l_q \end{bmatrix} - \tilde{u}_d \cdot \left(\begin{bmatrix} Il_d \\ -Il_q \end{bmatrix} + \begin{bmatrix} \tilde{i}l_d \\ -\tilde{i}l_q \end{bmatrix} \right) \tag{12}$$

$$\begin{bmatrix} pc_2 \\ qc_2 \end{bmatrix} = -(U_d + \tilde{u}_d) \cdot \begin{bmatrix} \tilde{i}l_d \\ -\tilde{i}l_q \end{bmatrix}. \tag{13}$$

Therefore, the difference between (12) and (13), which represents the difference between the two control methods, can be expressed by

$$\begin{bmatrix} pc_1 \\ qc_1 \end{bmatrix} - \begin{bmatrix} pc_2 \\ qc_2 \end{bmatrix} = -\tilde{u}_d \cdot \begin{bmatrix} Il_d \\ -Il_q \end{bmatrix}. \tag{14}$$

This relation (14) enables the difference in the performance of the AF's under nonideal mains voltage conditions to be understood. The powers shown in (14) constitute additional disturbances compared with the i_d-i_q method, and their contribution is significant due to the product of voltage oscillations by the average current components. Also, another performance decrease factor may arise for the p-q method if the oscillatory values in voltage and currents shown in (12) contain harmonics of the same order, resulting in additional average power components. In conclusion, it can be stated that under balanced and sinusoidal voltage conditions both methods have the same performance. Under any other voltage conditions the average and oscillatory powers are disturbed by voltage harmonics and unbalanced voltage conditions, so neither method achieves total harmonic elimination. However, in spite of the error introduced in the determination of power components, the i_d-i_q method performance is always superior compared with the p-q method under unbalanced and nonsinusoidal voltage conditions. Comparative results will be shown in further sections.

D. Steady State Analysis

The performance of the AF in steady state conditions is evaluated by simulation using the FFT algorithm, considering voltage and current variables as discrete sequences. A detailed description is presented in [8]. Applying the transformations given in Sections II-A and II-B new voltage, current and power variables are obtained. Since they now represent periodic sequences the FFT can be applied. Ideal and real filtering are used. In ideal filtering the average power and current components are eliminated. In real filtering, a Butterworth type filter is chosen, which is in accordance with the experimental prototype. This particular filter type was chosen, in order to obtain magnitude and phase characteristics as close as possible to an ideal filter since its magnitude response is maximally flat in the passband and is monotonic in both passband and stopbands. The filter considered is a fourth-order filter with a cutoff frequency $f_c = f/2$ ($f = 50$ Hz) which assures the elimination of dc components in the nonlinear load powers and currents.

The transfer function, $H(s)$, for an analog n-order Butterworth type HPF is

$$H_{\mathrm{HPF}}(s) = \frac{1}{\prod_{j=1}^{n} \left(\frac{\omega_c}{s} - s_j \right)}, \quad s_j = e^{j\pi\left[\frac{1}{2} + \frac{2j-1}{2n}\right]}. \tag{15}$$

To minimize the influence of the HPF's phase responses, an alternative HPF (AHPF) is obtained by mean of a low-pass filter (LPF) of the same order and cutoff frequency, simply by the difference between the input signal and the filtered one, which is equivalent to performing $H_{\mathrm{AHPF}}(s) = 1 - H_{\mathrm{LPF}}(s)$. The transfer function of the LPF can be derived by (15) exchanging the s and ω_c variables. Applying a discrete Fourier transform (DFT) of the filter impulse response to power and current spectra and calculating the inverse FFT (IFFT) the compensation currents are obtained. The performance of both control methods and filter effectiveness is evaluated again using the FFT over the source line currents. The performance criterion is measured by means of the average of Total Harmonic Distortion (THD) over the source currents, Is_{inh}, (16)

$$\mathrm{THD} = \frac{1}{3} \sum_{i} \frac{\sqrt{\sum_{n=2}^{25} Is_{inh}^2}}{Is_{i1h}}. \tag{16}$$

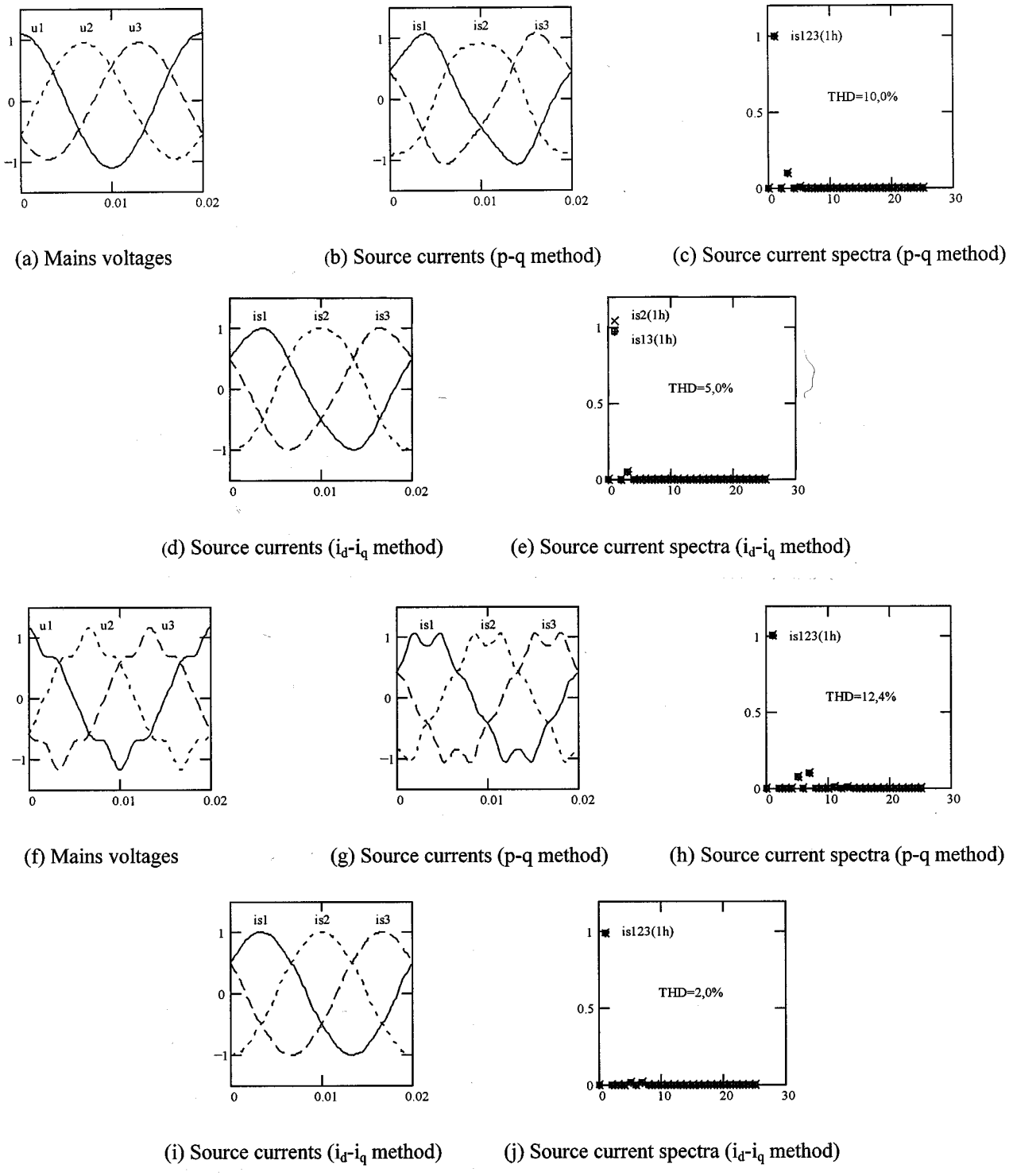

Fig. 3. AF performance under unbalanced and sinusoidal voltage conditions. (a) Mains voltages. (b) Source currents and (c) spectra for the p-q control method, $\mathrm{THD} = 10.0\%$. (d) Source currents and (e) spectra for the i_d-i_q control method, $\mathrm{THD} = 5.0\%$. AF performance under balanced and nonsinusoidal voltage conditions. (f) Mains voltages. (g) Source currents and (h) spectra for the p-q control method, $\mathrm{THD} = 12.4\%$. (i) Source currents and (j) spectra for the i_d-i_q control method, $\mathrm{THD} = 2.0\%$.

For simulation purposes the nonlinear load is a three-phase full converter. It is assumed that the thyristor rectifier ac currents are independent of the mains voltages and is operating under continuous dc current mode with a small ripple on its dc side. Considering a maximum harmonic order of 25 and a firing angle of 60° the rectifier currents present a THD value of 29.0%. The AF performance is analyzed under various mains voltage conditions. Under balanced sinusoidal voltage conditions a first harmonic system of positive sequence is considered. In the case of unbalanced sinusoidal voltage conditions a 10% first harmonic system of negative sequence related to the first harmonic is assumed. Finally, for the balanced nonsinusoidal voltage case the

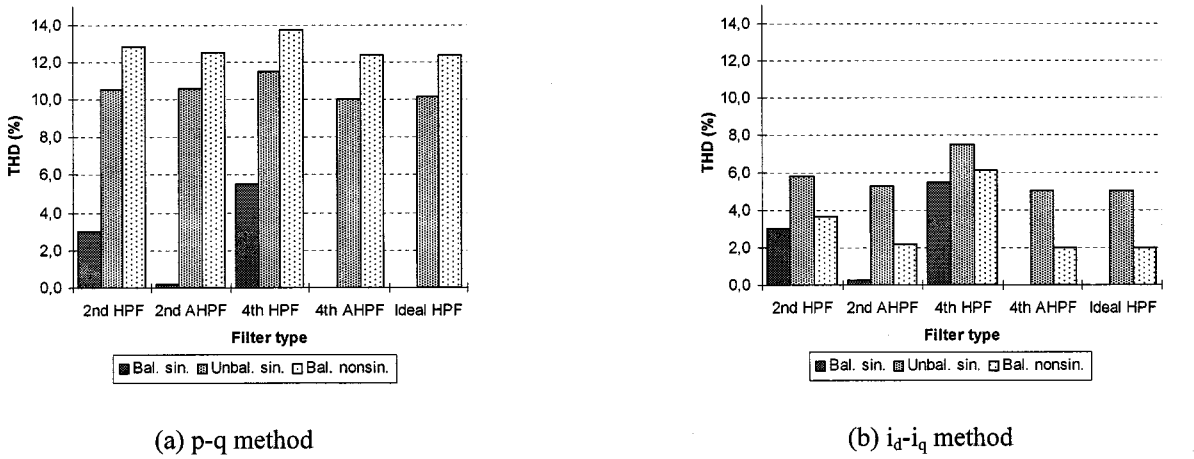

Fig. 4. Source current THD values. (a) p-q control method. (b) i_d-i_q control method.

systems considered are: a first harmonic of positive sequence, a fifth harmonic of negative sequence and a seventh harmonic of positive sequence with, respectively, $1/10$ and $1/14$ amplitude also related to the first harmonic.

Fig. 3(a)–(j) show the steady state behavior of the AF based on the p-q and i_d-i_q control methods for ideal filtering under nonideal mains voltages.

The bar graphs shown in Fig. 4(a) and (b) summarize the THD values for the two control methods as a function of mains voltage conditions and filter types.

The results presented in Fig. 4(a) and (b) confirm that for an ideal HPF the instantaneous active and reactive current component i_d-i_q method and the instantaneous active and reactive power p-q method attain a total harmonic compensation under balanced and sinusoidal voltage conditions. For the p-q control method a mains current balanced system is always obtained [Fig. 3(c)]. Under unbalanced voltage conditions the i_d-i_q control method generates a small unbalance in the mains currents [Fig. 3(e)]. In the two control methods the most severe cases are different. For the p-q control method the worst case is verified under nonsinusoidal mains voltages since the harmonic voltage content contributes to the average power values. By contrast, the worst case for the i_d-i_q control method is seen under unbalanced voltage conditions. It can therefore be concluded that low frequency oscillations in the direct voltage component caused by voltage unbalance may have a high impact on the decrease of AF performance. Under nonideal voltage conditions this last case is worse than the high frequency oscillations caused by voltage harmonics. Nevertheless, under unbalanced or nonsinusoidal voltage conditions the i_d-i_q control method always gives better results by presenting small values of THD. Among the filters used, it can also be verified that the best performance is achieved with a fourth-order AHPF [Fig. 4(a) and (b)].

III. System Control and Modeling

The AF proposed in Fig. 5(a) is based on the instantaneous active and reactive current component i_d-i_q method. The experimental prototype is a 2-kVA IGBT rated VSC. For the sake of simplicity, robustness, and good dynamics, in spite of some well-known disadvantages, the current controller used is composed of three independent two-level hysteresis comparators operating on a 3-leg VSC. This current controller enables the injection of the reference currents ic_i^* or ic_{dq}^* through the direct Park transformation. The converter currents ic_d^* and ic_q^* are obtained from the dc voltage regulation and harmonic current generation system presented in Fig. 5(b).

The system rating values considered in the AF are: mains (rms) voltage $U = 50$ V, inductance $L = 2.2$ mH, current hysteresis band, $H = \pm 0.25$ A, dc bus voltage $e_{\rm dc} = 175$ V. These parameters were chosen to give a compromise between a good transient response of the AF and low switching frequency. The maximum switching frequency verified experimentally was 18 kHz.

A. Harmonic Current Generation

By the inverse Park transformation the first harmonic load current of positive sequence is transformed to dc quantities, il_{dq1h}^+. These represent the harmonic current system that must be preserved in the mains. The ac components of the load current must be injected by the AF. These ac quantities are il_{dqmh}, which derive from the load currents il_{dq} through the AHPF presented in Fig. 5(b). Low-pass Butterworth fourth-order switched-capacitor filters are used. The cutoff frequency chosen is $f_c = f/2$. This assures a small phase shift in harmonics and a sufficiently fast transient response in the AF harmonic compensation.

As stated in Section II-D the fourth-order AHPF gives the best performance. Fig. 5(c) clearly shows that, although the AHPF presents four times less slope in the rejection band than the HPF (80 dB/dec), its phase response is very close to zero in the harmonic load current spectra. This is very important especially in the compensation of low frequency current components (e.g. second order harmonic current of negative sequence).

B. dc Voltage Regulation

A proportional-integral (PI) controller with anti-windup performs the voltage regulation on the VSC dc side. Its input is the capacitor voltage error $e_{\rm dc}^* - e_{\rm dc}$. Through regulation of the first

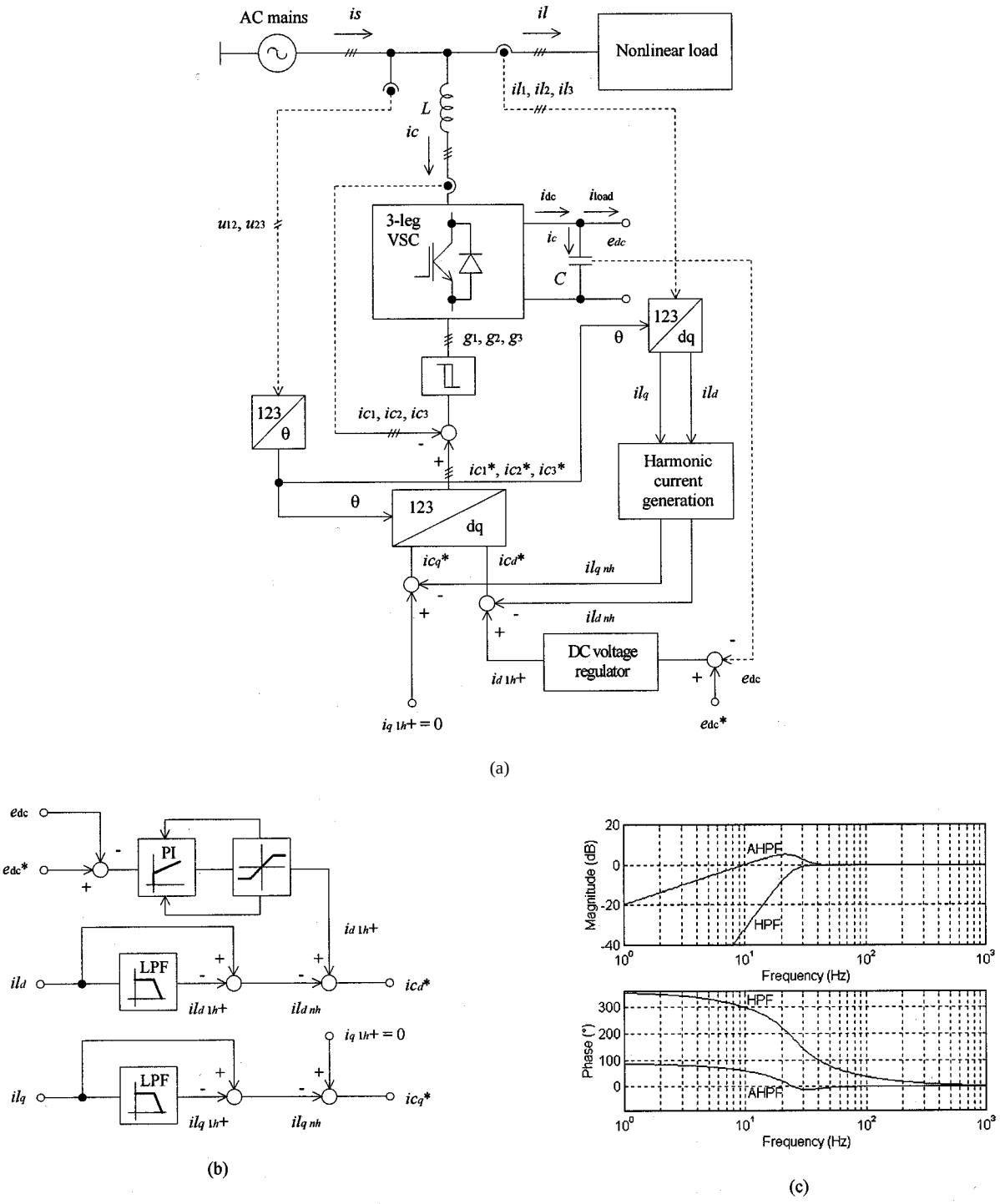

Fig. 5. (a) AF control system based on the instantaneous active and reactive current component i_d-i_q method. (b) dc voltage regulation and harmonic current generation system. (c) Magnitude and phase responses of an HPF and fourth-order AHPF.

harmonic direct current of positive sequence i^+_{d1h} it is possible to control the active power flow in the VSC and thus the capacitor voltage $e_{\rm dc}$. The reactive power flow may be controlled by the first harmonic quadrature current of positive sequence i^+_{q1h}. However, considering that the primary end of the AF is simply the elimination of current harmonics caused by nonlinear loads, the current i^+_{q1h} is set to zero.

As described above, the direct voltage component u_d is always equal to the amplitude of the voltage space vector. Under balanced sinusoidal voltage conditions $u_d = \sqrt{3}U$, where U is the mains RMS voltage. Assuming that the active power flow between mains and the VSC is equal to the active power on the dc side, i.e., ignoring the losses in the inductance and switching devices, then $p = u_d ic_d \approx e_{\rm dc} i_{\rm dc}$, where the variable $i_{\rm dc}$ is the

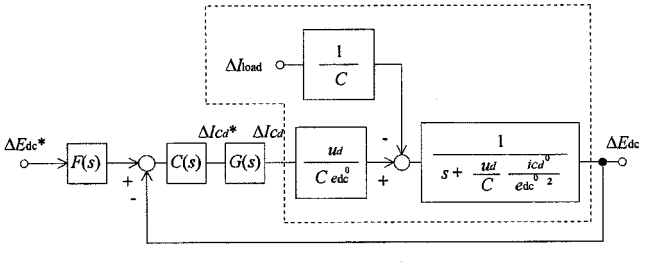

Fig. 6. Block diagram of the dc voltage regulation system.

current in the capacitor C. Thus, the state equation for the capacitor voltage is

$$\frac{de_{\rm dc}}{dt} = \frac{u_d}{C}\frac{ic_d}{e_{\rm dc}} - \frac{i_{\rm load}}{C}. \tag{17}$$

The current $i_{\rm load}$ is an extra load on the dc side of the VSC. Equation (17) is nonlinear, so, after performing a linearization about the operating point defined by $e^0_{\rm dc}$ and ic^0_d, the voltage regulation system is obtained (Fig. 6). Blocks $C(s)$ and $G(s)$ are the transfer functions (TF's) of the PI controller and the current control system, respectively. A filter $F(s)$ is used to eliminate the influence of the zero introduced by the PI controller in the forward-path TF, and consequently in the dc voltage regulation system closed-loop TF.

Based on Fig. 6 the dc voltage regulator $C(s)$ is synthesized assuming a unitary transfer function for $G(s)$ since its dynamics is far exceeded by the current control system dynamic. It is also assumed that there is no disturbance, i.e., the absence of an extra load at the capacitor. Under these conditions and considering the variables k_P and k_I as the proportional and integral gains of the PI controller, and $F(s)$ as a first-order low-pass filter with a gain of k_I/k_P and pole at $s = -k_I/k_P$, the closed-loop TF is

$$\frac{\Delta E_{\rm dc}}{\Delta E^*_{\rm dc}} = \frac{\frac{k_I u_d}{C e^0_{\rm dc}}}{s^2 + \frac{u_d}{C e^0_{\rm dc}}\left(\frac{ic^0_d}{e^0_{\rm dc}} + k_P\right)s + \frac{k_I u_d}{C e^0_{\rm dc}}}. \tag{18}$$

With a null active power flow in the converter, $ic^0_d = 0$, the closed-loop TF (18) is simplified. The design of the PI controller is realized by verifying that the simplification of (18) is a prototype second-order system. The variable values considered are: damping ratio $\zeta = \sqrt{2}/2$, natural undamped frequency; $\omega_n = \omega$, $(\omega = 2\pi f)$, dc bus capacitor $C = 2$ mF, dc voltage operating point $e^0_{\rm dc} = e^*_{\rm dc} = 175$ V. The magnitude and phase responses of the simplified closed-loop TF, and also the pole-zero map for a large variation in the current operating point $(-18\ {\rm A} < ic^0_d < 18\ {\rm A})$ in (18), are shown in Fig. 7.

The validity of the simplified model assumed (18) and the PI controller synthesis is valid due to the small variations in the pole locations even under a large variation in ic^0_d. As all the roots lie in the left-half s-plane the asymptotic stability is guaranteed. An experimental result is shown in Fig. 8(a) that also confirms the system stability through the system response to a step change $i_{\rm load} = 2.5$ A.

From Fig. 8(a) it is clear that the steady-state error obtained is null. The absence of steady-state error relative to a large disturbance is due to the introduction of a pole at $s = 0$ in the system forward-path TF by the PI controller, making a type 1 system. As a consequence there is also a null steady-state error

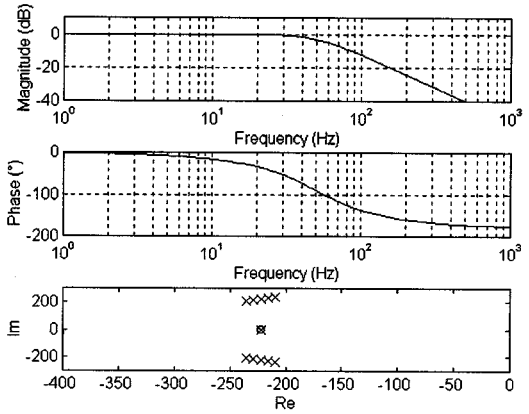

Fig. 7. Diagrams of the closed-loop TF $\Delta E_{\rm dc}/\Delta E^*_{\rm dc}$. Magnitude response, phase response and pole-zero map for a variation in the current operating point ic^0_d.

with respect to the disturbance variable on the VSC dc side. In conclusion, the results shown in Figs. 7 and 8(a) establish the validity of the system models used as well as the system stability considerations.

Fig. 8(b) presents an experimental result of the AF operating as a reactive compensator with reference currents $ic^*_d = 0$ A and a step change $ic^*_q = 10$ A. These results show an almost perfect decoupling between the d and q axes, since after a small perturbation the dc voltage remains constant. It should be noted that the current control system operates in closed-loop and its equivalent natural frequency is very high. All the experimental results shown in Fig. 8 are based on the AF topology presented in Fig. 5.

C. Park Transformation

A Park current calculator [10] performs the direct and inverse transformations described previously. In the experimental prototype the angle θ is calculated by (6), however u_α and u_β are derived form the mains line-to-line voltages u_{12} and u_{12} (19)

$$\begin{bmatrix} u_\alpha \\ u_\beta \end{bmatrix} = \sqrt{\frac{2}{3}} \cdot \begin{bmatrix} 1 & \frac{1}{2} \\ 0 & \frac{\sqrt{3}}{2} \end{bmatrix} \cdot \begin{bmatrix} u_{12} \\ u_{23} \end{bmatrix}. \tag{19}$$

The zero current components are null, therefore the inverse and direct Park transformations are obtained from (20) and (21), respectively

$$\begin{bmatrix} il_d \\ il_q \end{bmatrix} = \sqrt{2} \cdot \begin{bmatrix} \sin\left(\theta + \frac{\pi}{3}\right) & \sin(\theta) \\ \cos\left(\theta + \frac{\pi}{3}\right) & \cos(\theta) \end{bmatrix} \cdot \begin{bmatrix} il_1 \\ il_2 \end{bmatrix} \tag{20}$$

$$\begin{bmatrix} ic^*_1 \\ ic^*_2 \end{bmatrix} = \sqrt{\frac{2}{3}} \cdot \begin{bmatrix} \cos(\theta) & -\sin(\theta) \\ -\cos\left(\theta + \frac{\pi}{3}\right) & \sin\left(\theta + \frac{\pi}{3}\right) \end{bmatrix} \cdot \begin{bmatrix} ic^*_d \\ ic^*_q \end{bmatrix}. \tag{21}$$

In Fig. 9 a block diagram of the inverse Park current calculation and the Park current calculator implementation is presented. The measured voltages u_{12} and u_{23} pass through anti-aliasing filters and voltage limiters before digital conversion. Using two 8-bit semi-flash analog-to-digital converters (ADC's) a high conversion rate is achieved (sampling frequency $f_s = 200$ kHz). An address bus is established from the seven most significant bits of each ADC. The loss of 1 bit in the conversion is irrelevant since it represents noise and ADC error. The bus will address two 32 kb erasable programmable

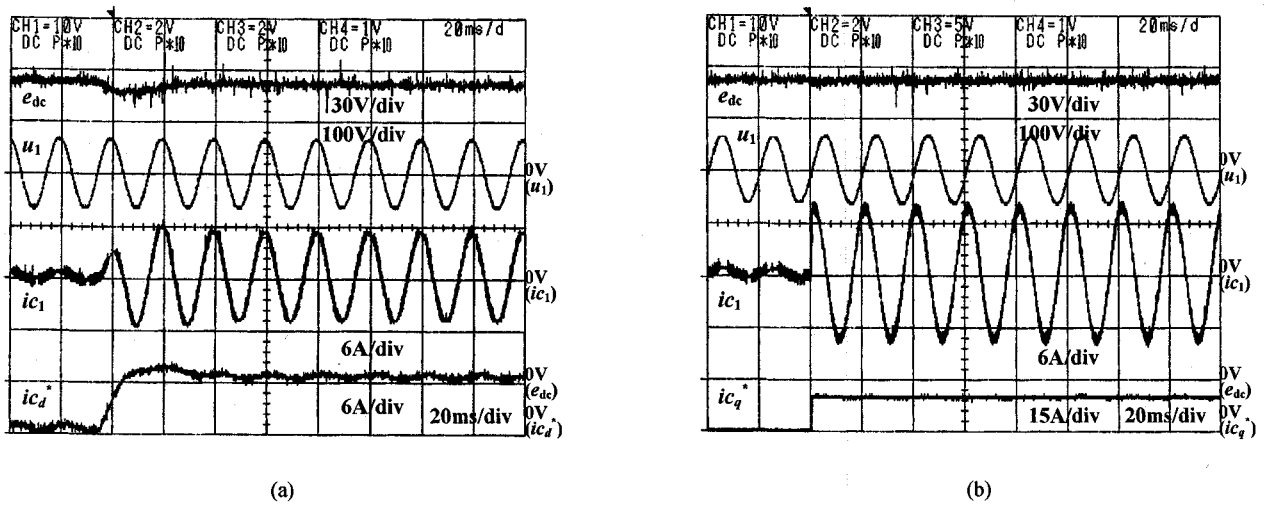

Fig. 8. (a) Experimental result of a step change $i_{\text{load}} = 2.5$ A. (b) Experimental result of a step change $ic_q^* = 10$ A.

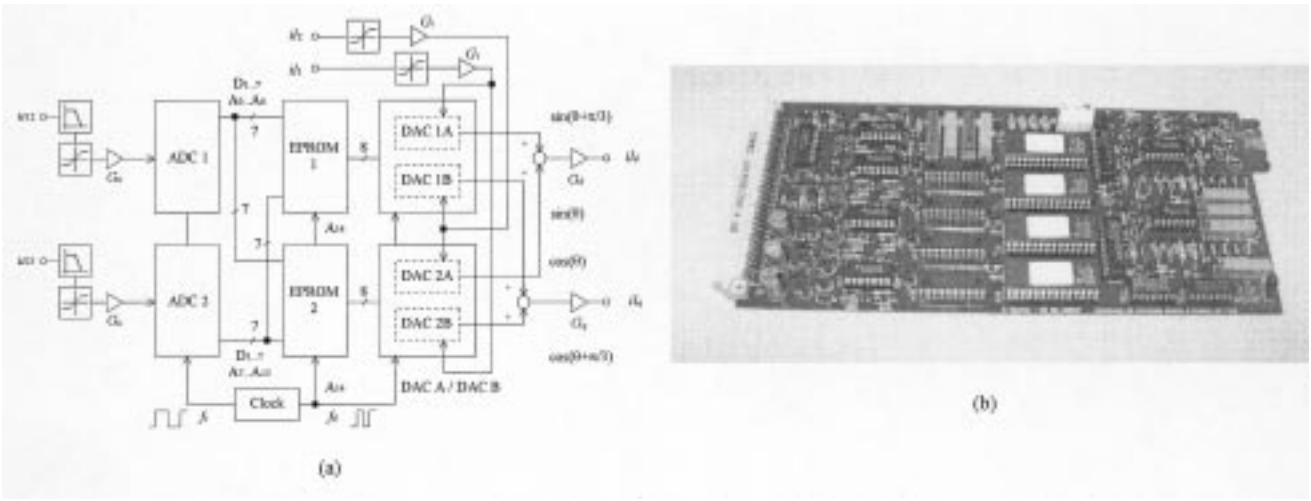

Fig. 9. (a) Inverse Park current calculation block diagram. (b) Laboratory implementation of the Park current calculator.

read-only memories (EPROM's) where the sinusoidal functions presented in (20) are stored. The outputs of the EPROM's are converted by two dual 8-bit 4-quadrant multiplying digital-to-analog converters (DAC's). The measured current values il_1 and il_2 are limited and multiplied by the DAC's. The sum of these signals gives the load currents il_d and il_q. The direct Park current calculation operates in a similar way, however the sinusoidal functions stored in the EPROM's are based on (21). In this case the result will be the VSC reference currents ic_1^* and ic_2^*.

Synchronization signals are obtained by a master clock built with a voltage-controlled oscillator and a D type flip-flop. These signals enable the sampling frequency to be established as well as the selection of the sinusoidal functions in the EPROM's since they are multiplexed. It also enables the proper selection of the 'read' and 'write' inputs in both ADC's and DAC's.

Although the Park current calculator circuit has been implemented using mixed analog-digital circuits, multiplications, divisions and square root operations are avoided which should be necessary if (7) and (8) were implemented. Moreover, using EPROM's as lookup tables all the trigonometric functions presented in (20) and (21) do not really need to be calculated. Significant computational time delays are overcome.

Low cost high speed operational amplifiers and DAC's enables to obtain a Park current calculator bandwidth of about 200 kHz with respect to the analog inputs. Another possible approach for the experimental implementation is the use of a digital signal processor (DSP). However, high-speed boards equipped with fast input/outputs and low execution time DSP's would be required in order to achieve a similar overall performance.

IV. System Performance

The AF steady state responses are presented in Fig. 10(a)–(i). The nonlinear loads considered are two type of thyristor rectifiers, being a three-phase full converter with firing angles $\alpha = 0°$ and $\alpha = 60°$, and a three-phase semiconverter with firing angle $\alpha = 60°$. All the rectifiers have a dc current of 10 A.

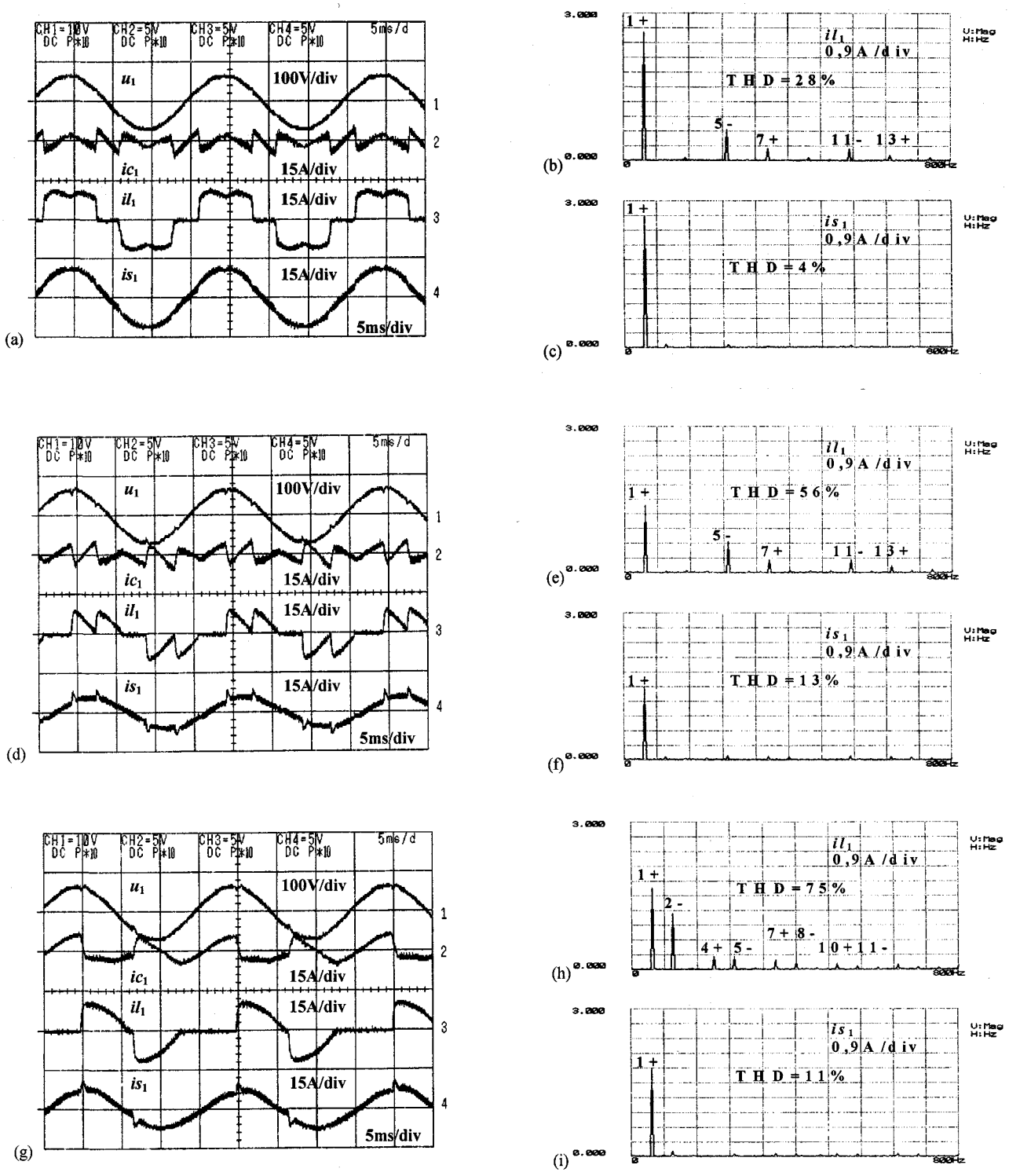

Fig. 10. Experimental results with a three-phase full converter with $\alpha = 0°$. (a) Voltage and current waveforms. (b) Load current spectra. (c) Source current spectra. Experimental results with a three-phase full converter with $\alpha = 60°$. (d) Voltage and current waveforms. (e) Load current spectra. (f) Source current spectra. Experimental results with a three-phase semiconverter with $\alpha = 60°$. (g) Voltage and current waveforms. (h) Load current spectra. (i) Source current spectra.

For balanced sinusoidal voltage conditions the experimental results show a significant decrease in THD of the mains current is_1 upon the injection of the compensation current ic_1. The mains current spikes shown in Fig. 10(d) and (g) are caused by fast transitions in load currents which cannot be compensated due to the limited bandwidth of the AF current control system. This situation occurs only with the three-phase full converter with $\alpha = 60°$ and with the three-phase semiconverter with $\alpha = 60°$, because the commutation effect appears near the peak voltage waveform where the di/dt is higher. Hence,

significant values of THD are obtained in these situations, as can be seen in Fig. 10(f) and (i). The situation presented in Fig. 10(g)–(i) is very demanding on the AF especially from the harmonic current generation system. The load current exhibits even and odd harmonics. There is also a second harmonic current of negative sequence, which is close to the cutoff frequency of the AHPF's. Overall, an average decrease in THD of a factor of six is achieved, corresponding to a high performance in harmonic current compensation.

V. Conclusion

An active filter based on the instantaneous active and reactive current component i_d-i_q method is proposed in this paper. Current harmonics of positive and negative sequence including the fundamental current of negative sequence can be compensated. The system therefore acts as a harmonic and unbalanced current compensator. A comparison between the instantaneous active and reactive current component i_d-i_q method and the instantaneous active and reactive power p-q method is realized. Under balanced and sinusoidal voltage conditions the control method proposed is identical to the instantaneous active and reactive power p-q method. Neither of the two control methods enables the current harmonics to be accurately compensated under unbalanced and nonsinusoidal conditions, nevertheless the i_d-i_q control method always leads to better results. The active filter compensation currents are generated by a three-leg VSC with hysteresis current control. A control system that enables current harmonics to be generated and the dc voltage to be regulated is implemented in Park coordinates. Expressions for the synthesis of the dc voltage regulator are derived and a stable and steady-state error free system is obtained. Experimental results from a 2-kVA IGBT prototype showing the transient and steady-state system performance are presented, where a high performance is achieved. The i_d-i_q control method proposed allows the operation of the AF in variable frequency conditions without adjustments. The compensation system can therefore work properly in a large frequency range covering both 50 Hz and 60 Hz three-phase distribution systems.

References

[1] H. Akagi, Y. Tsukamoto, and A. Nabae, "Analysis and design of an active power filter using quad-series voltage source PWM converters," *IEEE Trans. Ind. Applicat.*, vol. 26, pp. 93–98, Feb. 1990.

[2] S. Bhattacharya, D. Divan, and B. Banerjee, "Synchronous frame harmonic isolator using active series filter," in *Proc. EPE'91 Conf.*, vol. 3, 1991, pp. 30–35.

[3] C. Tuttas, "Sliding mode control of a voltage-source active filter," in *Proc. EPE'93 Conf.*, 1993, pp. 156–161.

[4] H. Akagi, "New trends in active filters," in *Proc. EPE'95 Conf.*, vol. 0, 1995, pp. 17–26.

[5] J. Tepper, J. Dixon, G. Venegas, and L. Morán, "A simple frequency-independent method for calculating the reactive and harmonic current in a nonlinear load," *IEEE Trans. Ind. Electron.*, vol. 43, pp. 647–654, Dec. 1996.

[6] V. Soares, P. Verdelho, and G. Marques, "Active power filter control circuit based on the instantaneous active and reactive current i_d-i_q method," in *Proc. PESC'97 Conf.*, vol. 2, 1997, pp. 1096–1101.

[7] L. A. Pittorino, J. A. du Toit, and J. H. R. Enslin, "Evaluation of converter topologies and controllers for power quality compensators under unbalanced conditions," in *Proc. PESC'97 Conf.*, vol. 2, 1997, pp. 1127–1133.

[8] V. Soares and P. Verdelho, "Analysis of active power filters in frequency domain using the fast Fourier transform," in *Proc. EPE'97 Conf.*, vol. 4, 1997, pp. 804–809.

[9] P. Verdelho and G. D. Marques, "An active power filter and unbalanced current compensator," *IEEE Trans. Ind. Electron.*, vol. 44, pp. 321–328, June 1997.

[10] V. Soares and P. Verdelho, "Instantaneous active and reactive current i_d-i_q calculator suitable to active power filters," in *Proc. PEMC'98 Conf.*, vol. 7, 1998, pp. 111–114.

Vasco Soares was born in Lisboa, Portugal, on March 26, 1969. He received the Dipl.Ing. degree in electrical engineering from the Instituto Superior de Engenharia de Lisboa in 1993, and the M.S. degree in electrical engineering from the Instituto Superior Técnico, Lisboa, in 1997, where he is currently pursuing the Ph.D. degree in active filters.

In 1993, he joined the Instituto Superior de Engenharia de Lisboa. Since 1999, he has been an Assistant Professor. His fields of study are active filters, static power conversion, instrumentation, and signal processing.

Pedro Verdelho (M'90) was born in Porto, Portugal, on December 26, 1963. He received the Dipl.Ing., M.S., and Ph.D. degrees from the Universidade Técnica de Lisboa-Instituto Superior Técnico, Lisboa, Portugal, in 1987, 1990, and 1995, respectively, all in electrical engineering.

He joined the Instituto Superior Técnico in 1985. Since 1995, he has been an Assistant Professor. He is also with the Entidade Reguladora do Sector Eléctrico, Portugal. His research interests include power electronics, active power filters, reactive power compensation systems, variable speed drive and generator systems, and power quality.

Gil D. Marques (M'81) was born in Benedita, Portugal, on March 24, 1958. He received the Dipl.Ing. and Ph.D. degrees in electrical engineering from the Technical University of Lisbon, Lisbon, Portugal in 1981 and 1988, respectively.

Since 1981, he has been with the Instituto Superior Técnico where he teaches electrical machines in the Department of Electrical and Computer Engineering. His research interests include electrical machines, static power conversion, variable speed drive, and generator systems, active power filters, and nonlinear dynamical systems.